The effects of Inverse Compton Losses on the Evolution of Electron Spectra from SNRs.

DESY Summer Student Programme, 2014

Leilee Chojnacki
NUIG, Ireland

Supervisor
Dr. Igor Telezhinsky

Group
THAT

4th of September 2014

Abstract

The electron energy losses due to Inverse Compton scattering on the radiation fields present around Type IIp SNRs are investigated. The target radiation field includes uniform CMB, galactic IR dust emission and background starlight from observations, and an originally modelled component accounting for HII recombination. The corresponding electron energy spectra evaluated for the free expansion stage of the SN reveal minor softening in the 0.1GeV to 100GeV range with respect to previously evaluated spectra taking into account only synchrotron losses by Telezhinsky et. al (2013).

1 Introduction

The origin of high energy cosmic rays is currently a major puzzle in modern astronomy and astrophysics, both in terms of locating signals from potential accelerators and in terms of modelling the variety of candidate objects and processes capable of their production.

The cosmic ray spectrum itself can be characterized by several regions dominated by different power laws; the power of the curve in any one region is called the spectral power index. More steeply decaying regions of the curve have higher spectral indices, and with respect to shallower parts of the curve are called softer, since these spectra favour more low energy particles. Conversely, when examining a more shallowly decaying region (lower spectral index) it is referred to as harder.

It is now thought that Supernova Remnants (SNRs) are the primary source of cosmic rays with energies below $3 \cdot 10^{15}$ eV[1]. At this energy, the cosmic ray spectral power index changes from roughly 2.7 to 3.0[1] -a feature known as the knee- resulting in a more steeply decaying spectrum for higher energies, that is , a softer spectrum. This change in power index could be indicative of the transition to a different mechanism dominating the acceleration, which is supported by the fact that simulated models of SNRs are unable to accelerate particles to energies beyond an upper limit of 10^{16} eV[2] and so other objects must be responsible for higher energy cosmic ray production.

Despite SNRs being considered strong candidates for producing these mid-range energy cosmic rays, current theoretical calculations -by way of simulations- produce spectra with harder spectral indices than observations: simulations produce an index near 2.0, which does not match the observed 2.7[1,3]. As a result, a major avenue of ongoing research is the adaptation of theoretical models to remove some of the simplifying assumptions, at the cost of increasing complexity of the problem and therefore computing time.

At DESY Zeuthen one such SNR simulation program called Patron (Particle Acceleration Transport Radiation Object-orieNted PYthon Code) is being developed by the THAT group to calculate -among other quantities- the expected spectra of electrons and protons accelerated in SNRs using the cosmic ray transport equation:

$$\frac{\partial N}{\partial t} = \boldsymbol{\nabla}(D_r \boldsymbol{\nabla} N - \mathbf{v}N) - \frac{\partial}{\partial p}((N\dot{p}) - \frac{\boldsymbol{\nabla}\mathbf{v}}{3}) + Q \tag{1}$$

where N is the number density of cosmic rays, the term in D_r pertains to cosmic ray diffusion, terms in $\mathbf{v}$ pertain to advection, the source term Q represents the injection of thermal particles into the acceleration process, and the term in $\dot{p}$ pertains to cosmic ray energy losses. The diffusion and advection terms are accounted for by hydrodynamical simulations within the program. The process of acceleration is modelled by diffusive shock acceleration. This mechanism relies on the fact that a particle crossing a shock front is always statistically more likely to undergo a head on collision with the particles on the other side of the shock: it is reflected back and forth acquiring energy each time, until it has acquired sufficient velocity to avoid the head on collisions responsible for reflection and is therefore able to escape; this results in the non thermal power law spectrum of index 2 mentioned above. The losses term at the start of this project accounted only

for synchrotron radiative losses, which are significant only for electrons due to their lower mass.

The objective of this project was to include the electron energy loss from Inverse Compton (IC) scattering on photons in the vicinity of the remnant and to see how the spectral index is modified. The following steps were taken in order to accomplish this:

(a) Patron was updated to include an IC losses term, with the interaction described by the relativistic cross section for photon-electron interactions, called the Klein Nishina (KN) cross section.

(b) The energy density of photons in the surroundings of the SNR was investigated to serve as the target field for the IC scattering of the non thermal spectrum of relativistic particles. Several sources of radiation were identified -which will be described in more detail in section 3- though only contributions from the first four have been successfully incorporated into Patron at the time of this report:

- Cosmic microwave background.
- Background starlight.
- Infrared galactic dust emission.
- Recombination spectrum from the HII clouds created by the star.
- Bremsstrahlung of the non thermal particles with the ionic clouds surrounding the remnant.

(c) The Patron simulation was then run to predict the evolution of electron spectra up to 400 years after a type IIp Supernova explosion.

2 Relativistic Inverse Compton effect

The Inverse Compton effect refers to photon-electron interactions in which the photon is upscattered to higher energies at the expense of kinetic energy from the electron in the laboratory frame. This process can be modelled identically to the Compton effect by using the electron rest frame, in which case from the relativistic Doppler effect[4] the incident photon energy becomes:

$$\epsilon = \epsilon' \gamma (1 + \beta \cos\theta) \tag{2}$$

For relativistic electrons β is approximately 1; additionally for isotropic photon density, $\cos\theta$ averages to 0. Under the latter assumption, the $(1 + \beta\cos\theta)$ factor can be set to 1, so for computational simplicity this has been omitted in the code.

It is worth noting that Patron works in terms of a normalized momentum component given by:

$$p_{norm} = \frac{p}{m_e c} = \gamma\beta \approx \gamma \tag{3}$$

The corresponding normalized photon energy is given by:

$$\epsilon = \gamma \frac{h\nu}{m_e c^2} \tag{4}$$

For a thermal distribution of photons this can be approximated instead by:

$$\epsilon = \gamma \frac{k_B T}{m_e c^2} \tag{5}$$

The scattering cross section for the relativistic Compton effect is given in terms of ϵ by the KN formula[5], which defines the interaction efficiency as a function of the energy of the photon in the electron rest frame (in gaussian units):

$$\sigma_{KN} = 2\pi \frac{e^2}{m_e c^2} \left[\frac{1+\epsilon}{\epsilon^2} \left(\frac{2(1+\epsilon)}{1+2\epsilon} - \frac{\ln(1+2\epsilon)}{\epsilon} \right) + \frac{\ln(1+2\epsilon)}{2\epsilon} - \frac{1+3\epsilon}{(1+2\epsilon)^2} \right] \tag{6}$$

The total power lost[6] by the electron via Inverse Compton scattering is equivalent to the power gained by the photon:

$$P_{IC} = \frac{4}{3} \sigma_{KN} c \gamma^2 \beta^2 U_{rad} \tag{7}$$

where U_{rad} is the photon energy density -or radiation field- investigated in the next section.

Combining the above with the non thermal power law momentum spectra generated by Patron allows electron spectra affected by the IC effect to be calculated. In order to confirm that the calculations are in line with expectation, a comparison was made between spectra affected by IC losses only and spectra affected by Synchrotron losses only. This comparison is reasonable given that the ratio of synchrotron power loss to IC power loss is just equivalent to the ratio of the corresponding target field energy densities (in cgs):

$$\frac{P_{IC}}{P_{syn}} = \frac{U_{rad}}{U_{mag}} = \frac{U_{rad}}{\frac{B^2}{8\pi}} \tag{8}$$

which is a manifestation of the fact that Synchrotron radiation is in essence the same type of scattering event as Compton scattering. We therefore expect the power losses to be equivalent for simulations scaled to have the same values for U_{rad} and U_{mag}. For this purpose, the magnetic field was modelled to be everywhere uniform and continuous with a value of 300μG. The equivalent U_{rad} field was therefore calculated to be:

$$U_{rad} = \frac{9 \times 10^{-8}}{8\pi} \approx 4 \times 10^{-8} erg/cm^3 \tag{9}$$

which is 10^{-4} orders of magnitude larger than the value for CMB (see section 3.1). The result of this comparison can be seen in Figure 1, and close examination shows the spectra lie directly on top of each other, demonstrating that the calculations for the IC losses are correct.

3 Target Radiation Fields

3.1 Background contributions

The background components of the radiation field surrounding the expanding remnant predominantly come from three different sources: the CMB, background diffuse starlight

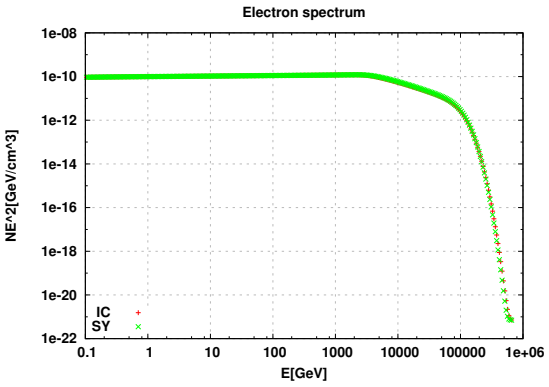

Figure 1: Diagnostic comparison of electron spectra produced with only IC (red) or Synchrotron (green) effects

and galactic IR dust emission. The background starlight can be further subdivided into two thermal blackbody fields to better capture the variety of spectral types of galactic stars: the first field is assumed to peak at 5000K and the second at 10000K. The CMB may be assumed to be isotropic, while for the other components the direction of the incident background depends heavily on the location of the star within the galactic plane. For simplicity, we shall assume a star deeply imbedded in the galaxy such that the incident light can be assumed to be isotropic -which is true at least for directions within the galactic plane- in order to make use of the argument followed in Section 2. Under this assumption, the quantity of interest for each component is the electromagnetic energy density U_{rad}. Values for each of these have been taken to be respectively $U_{CMB} = 4.0 \times 10^{-13}$ erg/cm^3, $U_{gIR} = 3.6 \times 10^{-13}$ erg/cm^3, $U_{5000} = 3.6 \times 10^{-13}$ erg/cm^3, and $U_{10000} = 3.6 \times 10^{-13}$ erg/cm^3[7].

3.2 HII Recombination

Stars with initial masses greater than 25 solar masses ($M_\odot$) burn initially with luminosities in excess of $110L_\odot$[8], which from the HR diagram yields a surface temperature on the order of 25000K. Once the star has reached the carbon burning phase, this value has risen to $140L_\odot$[8] though the star has migrated to the Giant branches, which leads to an equivalent surface temperature on the order of 5000K. The star's luminosity remains close to the latter value throughout the remaining stages of the star's life, and so too does the surface temperature.

The temperature of the star determines the number of ionizing photons it produces. If the star is hot enough it can ionize the circumstellar medium out to distances on the order of parsecs. This region would remain ionized while it is still bombarded by ionizing radiation from the star. Once its nuclear fuel is spent and the core collapse SN event occurs, the furthest reaches of the ionizing cloud beyond the SN shock front will recombine, releasing a recombination spectrum which -provided the recombination timescale is long enough- could contribute to the energy density of the IC target field. Let it be assumed for the moment that there is enough ionized material from the progenitor star at distances large enough to be downstream of the SN shock front. One further assumption must be made:

that the ionized medium is composed predominantly of Hydrogen, so its components are electrons and protons. This is called an HII region. To verify whether or not such a region could impact the cosmic ray spectrum through its recombinant radiation field, an estimate of the lifetime of the radiation field from this recombination can be made: the meantime per recombination is:

$$t_{recomb} = \frac{n_e}{\dot{N}_r} = \frac{n_p}{n_e n_p \alpha_n} = \frac{1}{n_e \alpha_n} \tag{10}$$

where n_e and n_p are the electron and proton number densities respectively, and α_n is the recombination coefficient for transitions from free-free state to levels of principal quantum number n. The recombination coefficients for n=1,2 and 3 dominate over the others; however it is reasonable to assume that all ground state recombinations, which result in the release of an ionizing photon, will be absorbed by any recombined surrounding atoms resulting in ionization. Therefore, there is no overall net release of energy into the radiation field by ground state recombinations. Using the value $12.4\times10^{-14}\mathrm{cm}^3/\mathrm{s}$[9] for the total recombination coefficient and taking average circumstellar electron and proton densities on the order of $10^3\mathrm{cm}^{-3}$ for an HII region (which typically range from 10 to $10^6\mathrm{cm}^{-3}$) gives a mean recombination time on the order of 255 years. This means that there could be recombination photons in the environment surrounding the SNR for at least several centuries after the death of the progenitor star, provided the star and its surrounding medium are suitable.

The next assumption that requires validation is that the extent of the HII region will exceed the SN shock front for the duration of the recombination timeframe, which roughly coincides with the duration of the free expansion phase of the remnant. The radius of the freely expanding remnant[10] is given by:

$$R_{shock} = \left(\frac{3M_0}{4\pi\mu m_h n_h}\right)^{1/3} \tag{11}$$

such that for a $25\mathrm{M}_\odot$, surrounding hydrogen density of $n_h = 1\ cm^{-3}$, and mean mass per hydrogen atom of $\mu = 1.2$, the radius works out to be on the order of 3.7pc.

The radius of the HII region can be approximated by the radius of a Strömgren sphere[11], determined based on the star's rate of production of ionizing photons:

$$R_{strömgren} = \left(\frac{3\dot{N}_{Ly}}{4\pi n_p n_e \sum_{n=2}^{\infty} \alpha_n}\right)^{1/3} \tag{12}$$

where the sum of values for alpha has been approximated to be equal to the contributions from the n = 2 and n = 3 recombination coefficients only. Assuming that the stellar spectrum is a perfect blackbody spectrum we can determine the production rate of ionizing photons to be:

$$\dot{N}_{ion} = 4\pi R_\star^2 \int_{\nu_{ion}}^{\infty} \frac{2h\nu^3}{c^2} \frac{1}{e^{-\frac{h\nu}{k_B T}}} \frac{1}{h\nu} \delta\nu \tag{13}$$

where the minimum frequency required to ionize neutral Hydrogen is $\nu_{ion} = 3.29\times10^{15}$ Hz (corresponding to 13.6eV), and contributions from lower energy photons can be considered negligible since the lifetimes of excited states of Hydrogen are on the order of 10^{-9}s[12], such that ionization from an excited state will not happen often enough to make a noticeable effect. The stellar radius of the $25M_\odot$ star during its Main Sequence phase is roughly $8R_\odot$[8], while during all burning stages from carbon onward this has drastically increased to $1000R_\odot$[8] since these phases take place on the Red Giant Branch. Substituting $x = \frac{h\nu}{k_B T}$ and $e^x - 1 = \sum_{n=1}^{\infty} e^{-nx}$, and evaluating this integral by partial fractions gives:

$$\dot{N}_{ion} = 4\pi R_\star^2 (\frac{k_B T}{h})^3 \frac{2}{c^2} \sum_{n=1}^{\infty} \left(\frac{x_{ion}^2}{n} + \frac{2x_{ion}}{n^2} + \frac{2}{n^3} \right) \tag{14}$$

Numerical evaluation up to n = 50 for a star of surface temperature 25000K leads to a production rate of 2.5×10^{50}s^{-1}, and remarkably for the 5000K phase the rate has increased to $7\times10^5 3$s^{-1}, in spite of the much cooler spectrum. This is due to the increase in the surface area of the star by a factor of almost 10^6. Using these values, the approximate radii of the HII regions during the early life of the star and at the end of its life are respectively 6.2pc and 88pc. The latter value is of course ludicrous, since in practice a star's influence is limited by the local characteristics of the Interstellar Medium, the local density of stellar population, etc. Yet this figure places an upper limit for the size of HII regions comfortably outside the SN shock radius, which validates the assumption that a contribution on the local radiation field from HII regions could be expected at all.

To evaluate the recombinant radiation density, the maximum energy expected to be released per timestep was defined as:

$$U_{recomb}(r,t) \approx n_p(r,t) n_e(r,t) \alpha_{2,3} X_{ion} t \tag{15}$$

where n_p(r,t) and n_e(r,t) are now the precise number densities as calculated from hydrodynamical simulations, X_ion = 13.6eV is the maximum energy released by cascade recombination and t is the timestep set as 1 year.

3.3 Bremsstrahlung

In the previous section it has been shown that Hydrogen in the medium surrounding the SN blast wave is completely ionized up to several parsecs away, the exact distance depending on the properties of both the progenitor star and the surrounding medium. This means that any charged particles escaping the shock front after being accelerated will undergo further Coulomb interactions in this ionized gas. As a result of the change in motion, these charged particles will transfer energy to the local radiation field by the same Larmor mechanism that underlies the IC power transfer, a process known as Bremsstrahlung or braking radiation. The parallel with Compton interactions can be highlighted by modelling the braking radiation as the interaction of electrons with the virtual photons of the Coulomb field: the same interaction cross sections apply. The analytical solution to non-thermal

electron bremsstrahlung emission has been found to be[13]:

$$\frac{dW}{dtd\omega dV} = \frac{16Z^2e^6}{3me^2c^4} n_i K_e (\xi_e \hbar\omega)^{1-q} \left(1 + 2\frac{m_e c^2}{\xi_e \hbar\omega}\right)^{1-\frac{q}{2}} \frac{1}{2} e^{Q(q-3)/2} \left[1 + \frac{e^Q - 2(2 + \frac{\xi_e \hbar\omega}{m_e c^2})}{(2 + \frac{\xi_e \hbar\omega}{m_e c^2})^2}\right]^{\frac{1}{2}} \left[\ln\left(0.684\xi_e(2 + \frac{\xi_e \hbar\omega}{m_e c^2})\right) + \frac{1/q}{1/q - 1}\right] \tag{16}$$

for photon energies -from the electron rest frame- residing within the non-relativistic Thomson interaction regime. At the time of this report, this expression is being recalculated to make use of the relativistic Klein Nishina interaction cross section. As such, neither the intirinsic losses from bremsstrahlung nor the corresponding increase in the radiant energy density have been incorporated into Patron.

4 Conclusions

The result of the simulated electron spectra evolution for type IIp Supernovae can be seen in Figure 2. Examination of the earliest spectra reveal minor softening in range from 0.1 GeV to 100 GeV as a result of energy losses with no corresponding energy gains elsewhere in the spectrum. At later ages, this range is shifted towards higher energies by a factor of roughly two over a period of 400 years.It is unclear whether this trend may continue to into the Sedov phase of evolution, for this purpose calculations could be extended to 2000 years. The methods used here can also by applied to other types of SNe, with the exception of the HII recombination model which requires a massive progenitor star destined to undergo a core-collapse event.

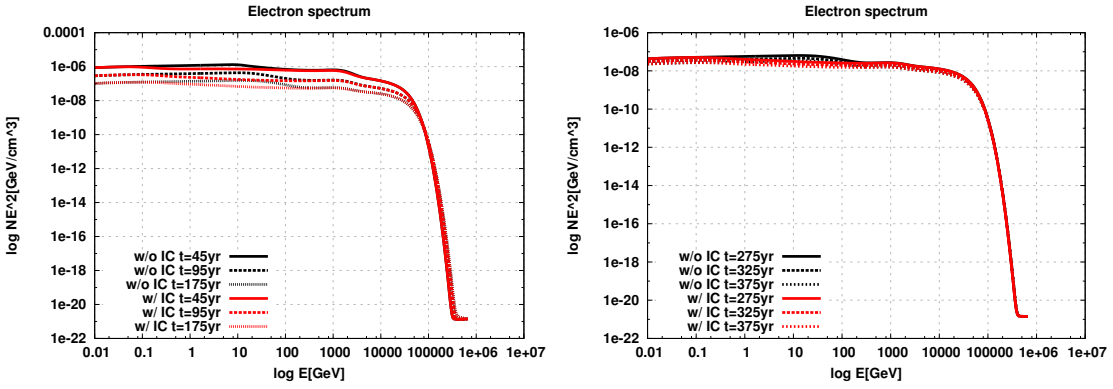

Figure 2: Electron spectra produced downstream by the SNR with and without IC losses at: (left) 0-200 years; (right) 200-400 years

References

[1] S.P. Reynolds, *Supernova remnants at high energies* Annual Review of Astronomy and Astrophysics **46**:89-126 (2008).

[2] J.G. Kirk, R.O. Dendy *Shock acceleration of cosmic rays - a critical review* J. Phys. G: Nucl. Part. Phys.**27** : 1589-1595 (2001)

[3] I. Telezhinsky, V. Dwarkadas, M. Pohl *Acceleration of cosmic rays by young core-collapse supernova remnants* Astronomy & Astrophysics **522** (2013).

[4] M. Harwit, *Astrophysical Concepts* (Springer, Third Edition, 1998), Equation 5-43.

[5] G. Rybicki, A. Lightman *Radiative processes in Astrophysics*, (WILEY-VCH, 2004) Equation 7.5.

[6] M.S. Longair *High Energy Astrophysics* (Cambridge University Press, 2nd edition, 1992).

[7] S.J. Sturner, J.G. Skibo, C.D. Dermer, and J.R. Mattox *Temporal evolution of non-thermal spectra from supernova remnants* The Astrophysical Journal **490**: 619-632 (1997).

[8] S.E. Woosley, A. Heger, and T.A. Weaver *The evolution and explosion of massive stars* Review of Modern Physics **74** (2002).

[9] M. Harwit, *Astrophysical Concepts* (Springer, Third Edition, 1998), Table 9.2.

[10] D. Lequeux *The Interstellar Medium* (Springer, 2005), Equation 12.1.

[11] M. Harwit, *Astrophysical Concepts* (Springer, Third Edition, 1998), Equation 9-9.

[12] W.S. Bickel, A.S. Goodman *Mean lifetimes of the 2p and 3p levels in atomic hydrogen* The Physical Review **148** (1966).

[13] V. Zeković, B. Arbutina, A. Dobardžić, and M. Pavlović *Relativistic non-thermal bremsstrahlung radiation* International Journal of Modern Physics A (2013).

[14] A.B. Underhill *Wolf-Rayet Stars: Observations, Physics, Evolution* 1982, pp 47-51.

[15] R.J. Gould, *Energy loss of relativistic electrons and positrons traversing cosmic matter* The Astrophysical Journal **196**: 689-694 (1975).

[16] J. Schwinger, L. DeRaad, Jr., K. A. Milton and W. Tsai, *Classical Electrodynamics* (Perseus Books, 1998).

[17] T. Padmanabhan *Theoretical Astrophysics, Volume I: Astrophysical Processes* (Cambridge University Press, 2000).